

A FLEXIBLE BEAM ACTUATED BY A SHAPE MEMORY ALLOY RIBBON

Veturia CHIROIU, Ligia MUNTEANU

¹Institute of Solid Mechanics, Romanian Academy
Corresponding author: veturiachiroiu@yahoo.com

The paper analyses the thermomechanical coupling between a cantilever aluminium beam and an embedded SMA ribbon. The SMA is selected to be Nickel-Titanium (NiTi) because of the high strength and large strains associated with this material. The actuation of the beam is achieved by applying a current across the SMA ribbon in order to heat the beam above the transition temperature. We show that the actuated beam exhibit the essential functions of an active system, i. e. the deflected beam may return to the initial configuration.

Key words: shape memory alloys (SMA), phase transformation, composites, active system.

1. INTRODUCTION

In the 1960s were developed some nickel-titanium alloys with a composition of 53-57% nickel by weight, that exhibited an unusual effect: the deformed specimens with residual strains of 6-10% regained their original shape after a thermal cycle. This effect became as the shape-memory effect. Shape memory alloys (SMA) are materials capable of very large recoverable inelastic strain (of the order of 10%). The source of this mechanical behavior is a crystalline phase transformation between the austenite and martensite. Martensitic structure is obtained from austenite with application of mechanical load or decrease in temperature. Upon heating or reduction of stress, the austenitic structure is recovered. In absence of stress, the start and finish transformation temperatures are typically denoted as M_s , M_f , A_s , A_f ($M_f < M_s < A_s < A_f$).

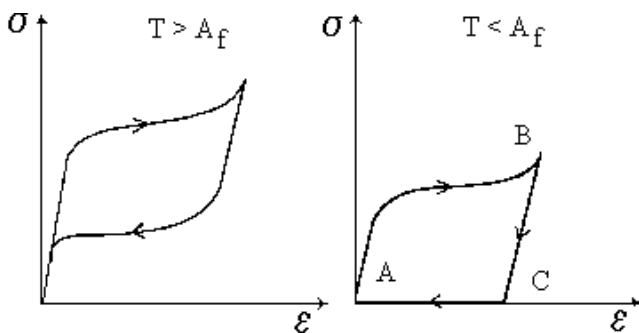


Fig. 1. Pseudoelasticity
(a) and shape memory effect
(b) for a SMA material
(after Brocca, Brinson and Bazant [1] 2002).

To illustrate the macroscale manifestation of these phenomena, typical uniaxial stress-strain diagrams for a polycrystalline SMA material are shown in Fig. 1 (after Brocca, Brinson and Bazant [1] 2002). At a temperature $T > A_f$, a SMA material behaves pseudoelastically (Fig.1a). Applying stress induces transformation of austenite into martensite, resulting in inelastic transformation strain.

As the stress is reduced, after an initial elastic response the martensite formed during the loading process transforms back to austenite, the inelastic strain is therefore recovered, and the stress-strain diagram exhibits the characteristic hysteresis loop shown in Fig. 1(a). Fig. 1(b) illustrates the shape memory effect

for material starting as austenite at a temperature $T < A_s$. During the loading process (A-B), the applied stress induces formation of martensite and inelastic strain. Upon unloading from B to C, the newly formed martensite remains stable, as does the transformation strain. Upon heating the material to temperatures above A_f , the material becomes again completely austenitic and the inelastic strain is fully recovered (C-A).

Martensite formed in such a manner assumes a self-accommodated structure in which the combination of variants does not produce a macroscopic observable strain. The stress applied to a martensitic structure induces a large, macroscopic deformation due to reorientation of martensite variants. When the temperature is increased again $T > A_f$, the martensite gradually transforms back to austenite with the original crystallographic orientation, thus allowing for a full recovery of the deformation.

The temperature at which the alloy remembers its high temperature form when heated can be adjusted by slight changes in alloy composition and through heat treatment. In the NiTi, for instance, it can be changed from above $+100^\circ\text{C}$ to below -100°C .

In this paper we consider the 2D bending problem of a cantilever flexible beam with an embedded ribbon of NiTi (55% Ni, 45%Ti) in an aluminium matrix. Both the rod and the actuator are assumed to be initially straight at $t = 0$ and $T_0 = 33^\circ\text{C}$. The NiTi ribbon is heated above the austenitic start temperature by passing an electrical current, and the deflected beam tends to return to the initial configuration. The NiTi alloy acts as an actuator transforming electrical energy into mechanical energy, annihilating the deformed shape of the rod.

2.FUNDAMENTAL EQUATIONS

Consider homogeneous isotropic thermally conducting elastic thin rod at uniform absolute temperature T_0 in the undisturbed state, with length L , width d and thickness h . A ribbon of NiTi of length L , width d and thickness h_0 is embedded into aluminium matrix (fig. 2). The fundamental equations for such a medium are written in the spirit of Nowinski [3] 1978, Boyd and Lagoudas [4], 1994, Shu, Lagoudas, Hughes and Wen [5] 1997, Rogers, Liang and Barker [7] 1989, Lagoudas and Tadjbakhsh [8] 1993, Dickey and Roseman [9] 1993. We use the summation convention throughout. A superposed dot denotes differentiation with respect to time while a comma is used for material derivatives.

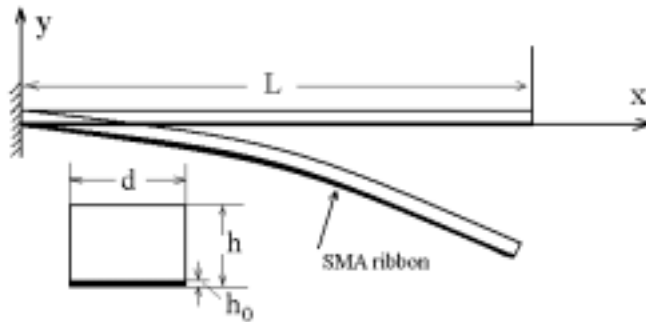


Fig. 2 The geometry of the beam

The fundamental equations are:

a. The constitutive law for an isotropic beam:

$$\sigma_{ij} = \lambda \varepsilon_{kk} \delta_{ij} + 2\mu \varepsilon_{ij} - \beta \delta_{ij} (T - T_0), \quad i, j, k = 1, 2, \quad (2.1)$$

where σ_{ij} are components of the stress tensor, ε_{ij} components of the strain tensor, T absolute temperature, T_0 initial temperature, λ, μ elastic Lamé's constants, $\beta = (3\lambda + 2\mu)\alpha$, with α the coefficient of linear thermal expansions.

b. The constitutive law for the SMA

$$\sigma_{ij} = \lambda_a (\epsilon_{kk} - \epsilon'_{kk}) \delta_{ij} + 2\mu_a (\epsilon_{ij} - \epsilon'_{ij}) - \beta_a \delta_{ij} (T - T_0), \quad i, j, k = 1, 2, \quad (2.2)$$

where ϵ'_{ij} are the transformation strain, and $\beta_a = (3\lambda_a + 2\mu_a)\alpha_a$. The Lamé moduli λ_a, μ_a and the coefficient of linear thermal expansions α_a obey the rule of mixtures:

$$\lambda_a = \lambda^A + \xi(\lambda^M - \lambda^A), \mu_a = \mu^A + \xi(\mu^M - \mu^A), \alpha_a = \alpha^A + \xi(\alpha^M - \alpha^A), \quad (2.3)$$

where the superscripts 'A' is for austenite and 'M' for martensite, respectively, and ξ is the current volume fraction of the martensitic phase.

c The motion equations:

$$\sigma_{ji,j} = \rho \dot{v}_i. \quad (2.4)$$

d The transformation strain rate evolution law:

$$\dot{\epsilon}'_{ij} = \Lambda_{ij} \dot{\xi}, \quad (2.5)$$

with the transformation tensor Λ_{ij} given by

$$\Lambda_{ij} = \begin{cases} \frac{3}{2} H \frac{\sigma'_{ij}}{|\bar{\sigma}|} & \dot{\xi} > 0, \\ H \frac{\epsilon'_{ij}}{|\bar{\epsilon}'|} & \dot{\xi} < 0, \end{cases} \quad (2.6)$$

which provides the directions in which the transformation strains develop. Here, $H = \epsilon'_{\max}$, and:

$$\bar{\sigma} = \sqrt{\frac{3}{2} \sigma'_{ij} \sigma'_{ij}}, \quad \sigma'_{ij} = \sigma_{ij} - \frac{1}{3} \sigma_{kk} \delta_{ij}, \quad \bar{\epsilon}' = \sqrt{\frac{2}{3} \epsilon'_{ij} \epsilon'_{ij}}. \quad (2.7)$$

e The thermodynamic force Φ that controls the onset of the phase transformation:

$$\Phi = \sigma_{ij} \Lambda_{ij} + \frac{1}{2} \Delta a^1 \sigma_{ij} \sigma'_{ij} + \Delta \alpha_a \sigma_{ij} \delta_{ij} (T - T_0) + \rho_a \Delta a^4 T - \frac{\partial f(\xi)}{\partial \xi} - Y = 0. \quad (2.8)$$

In the above, ρ_a is the density of the SMA, $\Delta a^1 = \frac{1}{E^M} - \frac{1}{E^A}$, $\Delta \alpha_a = \alpha^M - \alpha^A$, $\rho_a \Delta a^4$ the difference of the entropy at the reference state, Y the threshold value of transformation, $f(\xi) = \frac{1}{2} \rho_a b_1 \xi^2$ provides the isotropic hardening term characterized by the isotropic hardening parameter b_1 .

The above criterion is valid for both reverse and forward transformation but with different values of the parameters $\rho_a \Delta a^4$, Y , b_1 which accounts for the hysteresis of shape memory alloys. During cooling we have

$$\rho_a \Delta a^4 = -C^M H, \quad Y = -C^M H M_{0s}, \quad \rho_a b_1 = C^A H (A_{0f} - A_{0s}). \quad (2.9)$$

During heating we have:

$$\rho_a \Delta a^4 = -C^A H, \quad Y = -C^A H A_{0f}, \quad \rho_a b_1 = C^M H (M_{0s} - M_{0f}). \quad (2.10)$$

In the above, C^M and C^A are the slopes of the curves of the stress versus temperature, M_{0s}, M_{0f}, A_{0s} and A_{0f} are the start and finish temperatures at zero stress.

f. The heat equation is:

$$\rho c (\dot{T} + \tau_0 \ddot{T}) + T_0 \beta (\dot{\epsilon}_{ii} + \tau_0 \ddot{\epsilon}_{ii}) = k T_{,ii}, \quad (2.11)$$

for the rod, and:

$$C_v(\dot{T} + \tau_0 \ddot{T}) + T_0 \beta_a (\dot{\epsilon}_{ii} + \tau_0 \ddot{\epsilon}_{ii}) = k_a T_{,ii} + \rho_e J^2, \quad (2.12)$$

for the ribbon, where $C_v = \rho_a c_a$ is the heat capacity, k_a the thermal conductivity, ρ_e the electrical resistivity and J the magnitude of the current density.

The equations of motion in displacements are obtained by substituting (2.1) or (2.2) in (2.4). So, we obtain:

$$\rho \ddot{u}_i = (\lambda + \mu) u_{j,ij} + \mu u_{i,jj} - \beta T_{,i}, \quad (2.13)$$

for the rod, and:

$$\rho_a \ddot{u}_i = (\lambda_a + \mu_a) u_{j,ij} + \mu_a u_{i,jj} - \beta_a T_{,i}, \quad (2.14)$$

for SMA, where u^t is the transformation displacement.

g. The boundary conditions for the beam:

$$\sigma_{22} = \sigma_0 \text{ at } x = L \text{ and } t \in [0, t_1]. \quad (2.15)$$

h. The conditions on the interfaces between the rod and ribbon:

$$[u_2] = [\sigma_{22}] = [\sigma_{12}] = 0, \quad t \in [0, t_1]. \quad (2.16)$$

3. SIMULATION OF THE STRUCTURAL RESPONSE

For solving the equations (2.11)-(2.14) under the conditions (2.5), (2.8), (2.15), (2.16) we use an integrable discretisation of the characteristic equations associated to these equations. This technique is obtained from the classical Bäcklund transformation (Coley, Levi, Milson, Rogers and Winternitz (eds.) 1999 [11], Rogers and Schief 1997 [6], Munteanu and Donescu 2002 [12]) and it is linked to the geometry of pseudospherical surfaces, in particular to Tzitzeica surfaces. The Bäcklund transformation gives a multi-parameter class of solutions of the associated integrable system. In terms of the eulerian coordinate $\bar{x} = \bar{x}(X, t)$, $\bar{x} = (x, y)$, $X = (X, Y)$:

$$d\bar{x} = (\varepsilon + 1)dX = vdt \quad (3.1)$$

so that $\rho_0 dX = \rho dx - \rho v dt$, we obtain two Monge-Ampère generalized equations. Once a solution of these equations has been determined, the general solutions are given parametrically in terms of a minimal set of parameters (in this case two) to verify the boundary conditions. The Bäcklund transformation represents an integrable discretization of the non-linear characteristic equations of the Monge-Ampère generalized equations associated with the evolution equations. The results are well confirmed by the numerical solutions constructed by using FEMLAB.

The geometry of the aluminum beam and the material parameters are given in table 1. The material parameters of the NiTi ribbon are given in table 2 (subscripts s and f represent start and finish temperature with '0' standing for stress free state).

Table 1 Material parameters and geometric constants of aluminium bar

Parameter	Symbol	Value	Unit
length	L	1	m
width	d	0.1	m
thickness	h	1.6×10^{-3}	m
density	ρ	2.71×10^3	Kg/m^3
elastic Lamé moduli	λ	50.01	GPa
	μ	28.21	GPa
coefficient of linear thermal expansions	α	1.2×10^{-5}	$1/^\circ\text{C}$

Table 2 Material parameters of NiTi ribbon (after Ditman, White and Bergman [10])

Parameter	Symbol	Value	Unit
length	L	1	m
density	ρ_a	6.45×10^3	Kg/m^3
elastic Lamé moduli	λ^A, λ^M	28.26, 6.3	GPa
	μ^A, μ^M	18.85, 4.19	GPa
coefficient of linear thermal expansions	α^A, α^M	12.5×10^{-6}	$1/^\circ\text{C}$
thermal conductivity	k^A	18	$\text{W/m}^\circ\text{C}$
	k^M	8.5	
Slope of stress versus temperature	C^A	13.5	$\text{MPa}/^\circ\text{C}$
	C^M	13.5	
Transformation temperatures	A_{0s}, A_{0f}	57, 35	$^\circ\text{C}$
	M_{0s}, M_{0f}	21, -12	
Heat capacity	C_v	5.44×10^6	$\text{Jm}^{-3} \text{ }^\circ\text{C}$
Electrical resistivity	ρ_e	0.5×10^6	$\Omega \text{ m}$
Ribbon thickness	h_0	1.27×10^{-3}	m

Consider $t_1 = 25$ sec. At $t = 0$ and $T = 33^\circ\text{C}$ the beam is acted to an initially stress $\sigma_{22} = 350$ MPa at $x = L$ and $t \in [0, t_1]$. The NiTi ribbon is heated above the austenitic start temperature by passing an electrical current as shown in fig. 3.

The NiTi alloy acts as an actuator transforming electrical energy into mechanical energy, annihilating the deformed shape of the rod. It takes about 3.7 sec to heat up the section $x = L$ to the austenite finish temperature $A_f = 122^\circ\text{C}$ at stress $\sigma = 350$ MPa, and about 6 sec. to cool it down to martensitic finish temperature $M_{0f} = 33^\circ\text{C}$ at stress $\sigma = 0.004$ MPa.

The corresponding temperature and stress profiles at $x = L$ are shown in figs. 4 and 5.

A scheme of the tip deflection ($x = L$) with respect to ϵ'_{22} and temperature is shown in fig. 6.

Each trajectory of the tip point starts from a maximum value (left part of the graphic at $t = 0$ sec), decreases to zero (top of the curve at $t = 3.7$ sec), and increases again to its maximum value at $t = 9.7$ sec.

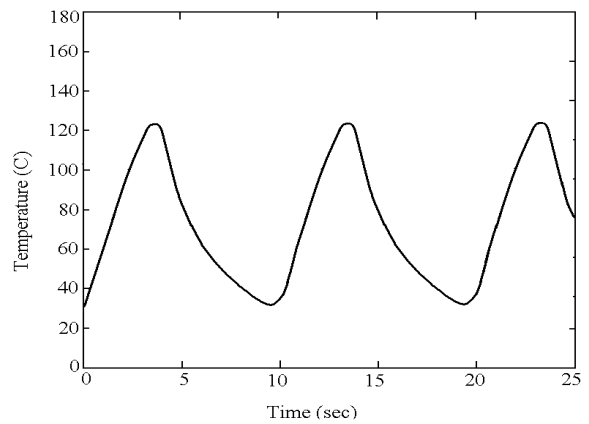
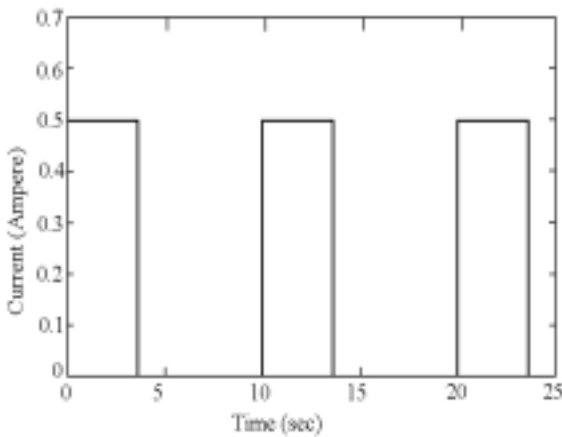


Fig. 4 Temperature-time profile of the beam at $x = L$

Fig. 5 On-off step input of the electrical current profile

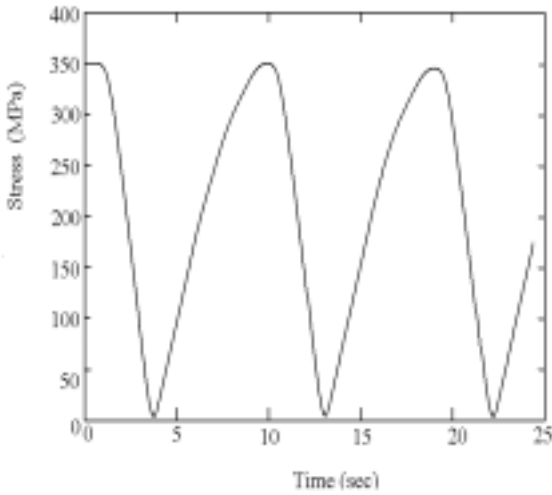


Fig. 5 Stress σ_{22} versus time profile of the beam at $x = L$

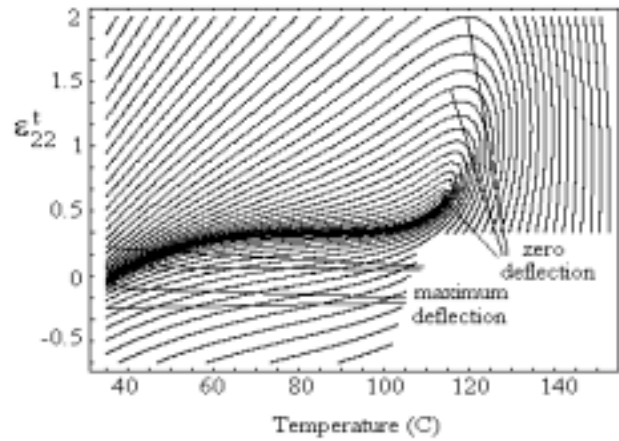


Fig. 6 Tip of the beam deflection with respect to ϵ_{22}^t and temperature

In closing, shape-memory alloys show features not present in materials traditionally used in engineering. So, they are the basis for innovative applications. For the example considered in this paper it is observed that $H = \epsilon_{\max}^t$ is 1.98%. Other features, such as the temperatures A_f and M_s , can also be captured by the thermodynamic model. It is found that for this specific case, the inelastic strain of the beam (35.7 % of its length) is completely recovered. In Fig. 7 a complete set of transformations is followed by a partial unloading-reloading cycles. A partial reloading implies an incomplete transformation austenite- martensite, while a partial unloading implies an incomplete reverse transformation. Fig. 7 describes a series of loops, which are internal to the complete loading-unloading cycle. Such internal loops present a ratcheting effect which stabilizes after a few cycles.

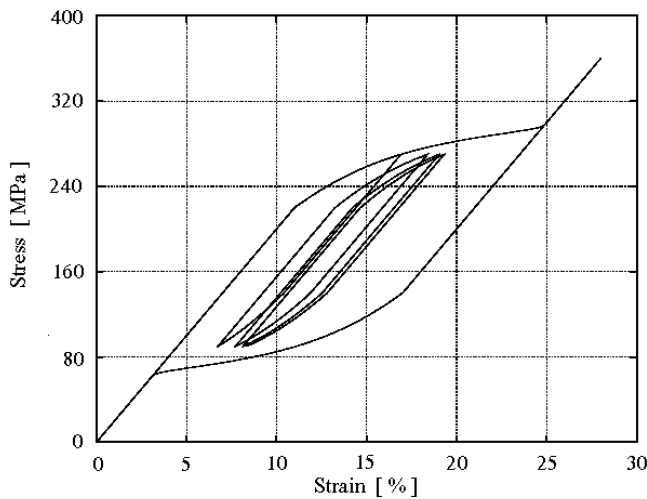


Fig. 7 Multiple stress cycles at constant temperature: stress σ_{22} versus strain ϵ_{22} .

Acknowledgement

The work reported here was supported by the Romanian Academy grant GAR nr. 60/2002 and the National University Research Council (NURC-CNCSIS) grant nr.33517/2002. A special acknowledgement goes to Dr. Eugen Soós for helping us in developing the new technique of solving the equations.

REFERENCES

1. BROCCA, M., BRINSON, L. C., BAZZANT, Z. P., *Three- dimensional constitutive model for shape memory alloys based on microplane model*, Journal of the Mechanics and Physics of Solids 50, p.1051 – 1077, 2002.
2. OTSUKA, K., WAYMAN, C.M., *Shape Memory Materials*, Cambridge University Press, Cambridge, 1998.
3. NOWINSKI, J. L., *Theory of thermo-elasticity with applications*, Suthoff & Noordhoff International Publishers Alphen Aan Den Rijn, 1978.
4. BOYD, J.G., LAGOUDAS, D.C., *Thermo- mechanical response of shape memory composites* J. Intell. Mater. Struct. 5, p.333–46, 1994.
5. SHU, S. G., LAGOUDAS, D. C., HUGHES D., WEN, J. T., *Modeling of a flexible beam actuated by shape memory alloy wires*, Smart Mater. Struct. 6, p.265–277, 1997.
6. ROGERS, C., SCHIEF, W. K., *The classical Backlund transformation and integrable discretisation of characteristic equations*, Physics Letters A 232, p.217-223, 1997.
7. ROGERS C., LIANG C., BARKER D., *Behavior of shape memory alloy reinforced composite plates* (part I and II), Proc. 30th Structures, Structural Dynamics and Materials Conf. Mobile, Alabama, 1989.
8. LAGOUDAS D.C., TADJBAKHSI I.G., *Deformations of active flexible rods with embedded line actuators*, Smart Mater. Struct. 2, p. 71–81, 1993.
9. DICKEY R.W., ROSEMAN J.J., *Equilibria of the thin elastic rod under a uniform central force field*, Quarterly of Applied mathematics, vol. LI, nr.2, june 1993.
10. DITMAN J, WHITE S.R., BERGMAN L., *Tensile testing of nitinol wire*, Technical Report UILU ENG 91-0508, University of Illinois, Urbana IL, 1991.
11. CRM Proceedings&Lecture Notes, *Bäcklund and Darboux Transformations. The Geometry of Solitons*, vol.20, AARMS-CRM Workshop, june 4-9, 1999, Halifax, N.S., Canada (A. Coley, D. Levi, R. Milson, C. Rogers, P. Winternitz (eds.)), American Mathematical Society, 1999.
12. MUNTEANU, L., DONESCU St. *Introducere Teoria solitonilor. Aplicatii Teoriei Mecanice*, Publishing House of the Romanian Academy, 2002.

Received June 3, 2002